Synthesis Characterisation of Nano-ZnO Particles by Chemical Reduction and their Application of Anti-Microbial Activity against some pathogens

Gundala Madan Kumar[1], Ginne Kalpana[3], M. Ravinder[2] and J.V. Shanmukha Kumar[1]*
1. Department of Chemistry, Koneru Lakshmaiah Education Foundation, Guntur-522502, Andhra Pradesh, INDIA
2. Chaitanya (Deemed to be University), Hanamakonda-506001, Warangal, Telangana, INDIA
3. Vaagdevi Engineering College, Bollikunta, Warangal, T.S., INDIA
*shanmukh_fed@kluniversity.in

Abstract

This study employed the chemical reduction (CR) method to synthesize nano-ZnO particles of varying sizes. $Zn(NO_3)_2$ functions as a metal precursor whereas $NaBH_4$ operates as a reducing agent, creating the fundamental elements necessary for the synthesis of nano-ZnO particles. The detailed chemical composition of nano-ZnO powders was examined through Fourier transform infrared spectroscopy (FTIR), X-ray diffraction (XRD), Scanning electron microscopy (SEM) and Transmission electron microscopy (TEM).

The analysis of the nano-ZnO particle encompassed an examination of its composition, shape, size and crystallinity. The nano-Zn oxide particles were measured at 100 nm and displayed a wurtzite hexagonal structure. The method employed for testing antibacterial activity against both Gram-positive and Gram-negative bacteria facilitated the assessment of the antimicrobial properties of the synthesized nano-ZnO particles.

Keywords: Nano-Zinc Oxide particles, Chemical reduction, FTIR, XRD, SEM, TEM and Anti-Microbial activity.

Introduction

Carbon nanomaterials represent the foundational and most exemplary manifestation of nanotechnology whereas metal nanosized particles, with Nano-Zn Oxide particles being among the most notable examples, illustrate this field's advancements. The dimensions of the nano-zinc oxide particles fall within the range of 1 to 100 nm. Metal nanoparticles exhibit variations in properties compared to bulk material which are influenced by their specific innovative applications[5]. Furthermore, nano-ZnO materials are classified within the II-VI group, exhibiting a significant energy band gap of E_0 = 3.4 eV and a high excitation energy of 60 eV. These properties enable them to endure strong electric fields, elevated temperatures and high-power operations[4].

Nano-ZnO particles have found utility in numerous applications including gas sensors, luminous oxides, rubber, ceramics, paints and more, due to their distinct physical and chemical properties[7]. Nano-Zn oxides are proposed for use in the food, cosmetic and pharmaceutical industries due to their exceptional purity and antimicrobial properties[2]. A variety of physical and chemical processes including the sol-gel technique, co-precipitation, ball milling, laser ablation, solvothermal and hydrothermal synthesis methods, have been employed to produce nano-Zn oxide particles, alongside CR[1,3,6,9].

FTIR, XRD, SEM and TEM represent a selection of the analytical techniques employed to investigate and characterize nano-Zn oxide particles[8]. The nano-Zn oxide particles examined in the previous study demonstrated a more pronounced inhibitory effect on both Gram-positive and Gram-negative bacteria.

Material and Methods

Materials: 98.0% $Zn(NO_3)_2$, 98.0% NaBH4, sodium alginate, 99.0% THF and deionized water, are analytical quality reagents from S.D. Fine Chemicals.

Method: The CR method was employed to produce the nano-ZnO particle[10]. 100 mL solution of 0.1 M $Zn(NO_3)_2$ was prepared by dissolving the compound in deionized water. This was followed by the preparation of 100 ml of 0.1 M $NaBH_4$ solution, which was dissolved in THF. Finally, a 100 ml solution of 10% sodium alginate was created by dissolving it in deionized water for the synthesis of nano-zinc oxide particles. In an RB flask, 50 mL of 0.1 M $Zn(NO_3)_2$ solution was added. The solution was heated to a temperature range of 60-70°C, with continuous stirring using a magnetic stirrer for approximately 60 minutes. This standard operating procedure requires execution under different dropping durations and reaction temperatures.

Following this, 20 ml of 10% sodium alginate solution was added dropwise with steady stirring after 50 ml of a 0.1 M $NaBH_4$ solution was added over 20–30 minutes. Maintain the entire reaction mixture at a temperature of 60–70°C for 180 minutes using a magnetic stirrer. At this stage, isolate the nano-zinc oxide precipitate which exhibits a light-yellow hue.

Results and Discussion

Scanning Electron Microscopy (SEM): The SEM data indicate that the particle size of nano-zinc oxide is 100 nm. Dynamic Image Analysis (DIA), a modern technique for particle characterization, was employed to determine size distributions and shape parameters. The surface shape is

observed to be spherical and amorphous as illustrated in figs. 1, 2, 3 and 4. The surface structure and size of nano-ZnO particles were confirmed through the chemical reduction method, as indicated by the data. The size of particles significantly influences the antibacterial and antimicrobial properties of zinc nanoparticles.

Transmission Electron Microscopy (TEM): The sample undergoes a TEM examination, yielding visual data regarding the nano-ZnO particles after the complete formation of the nano-ZnO film has been confirmed. Images are processed using ImageJ to determine the average particle size and generate a histogram of particle diameters. The use of electron diffraction in TEM allows for the precise determination of the orientation of nano-ZnO and the identification of its components. The study indicates that the data on nano-ZnO particles reveal morphological characteristics that are spherical and amorphous with particle sizes measuring 100 nm, as illustrated in figs. 5, 6, 7 and 8. In conclusion, the CR procedure leads to a reduction in particle size.

X-Ray Diffraction (XRD): Fig. 9 presents the findings from an X-ray diffractometer, confirming the presence of nano-sized ZnO powder along with its crystalline structure. The findings presented in fig. 9 indicate that the peaks occur at 31.77°, 34.44° and 47.60°. The synthesized nano-ZnO particle structure was confirmed to exhibit the hexagonal phase of ZnO, supported by the evidence and observed peaks. The XRD patterns exhibited broadened peaks which influenced the solid nano-ZnO material. The full width at half maximum (FWHM) of the diffraction peaks was used to determine the average crystalline size of the Nano-ZnO powdered material by applying the Scherrer equation. The XRD pattern indicated that the ZnO nanoparticles exhibited either a cubic or hexagonal wurtzite crystal structure, with an average crystallite size ranging from 100 to 200 nm, contingent upon the reaction time.

FTIR (Fourier transform infrared) Spectroscopy: Fig. 10 illustrates the wide absorption band peaks in the FTIR spectrum of nano-ZnO, which correspond to the stretching frequencies of the prominent hydroxyl group, C=O group, ammonium ion and C-H and C-O single bond stretching vibrations, as well as B-H stretching vibrations respectively. The observed peak positions are 3434.96 cm^{-1}, 1626.60 cm^{-1}, 1384.20 cm^{-1}, 2800-3000 cm^{-1}, 1111.06 cm^{-1} and 994 cm^{-1}. Furthermore, it facilitates the identification of a range between 600 and 720 cm^{-1} corresponding to C-H bending vibrations. The peak observed at 469 cm^{-1} corroborates the presence of nano-zinc oxide particles as indicated by the data and table 1.

Anti-Microbial Activity: This affects an antibiotic's capacity to suppress pathogen proliferation and the necessary dosage for patient treatment. The antimicrobial activity of Nano-ZnO particles produced by CR was quantitatively assessed using Muller-Hinton agar bacterial inoculum against the Gram-positive bacterium *Streptococcus pyogenes*, as well as the Gram-negative bacterium, *Pseudomonas aeruginosa* and *Klebsiella pneumoniae*. The synthesis of nano ZnO particle powder was validated through FTIR analysis, revealing that the resulting adsorbent exhibited an average pore size of 2.527 nm and an N_2 physisorption surface area of 113.751 $m^2\ g^{-1}$.

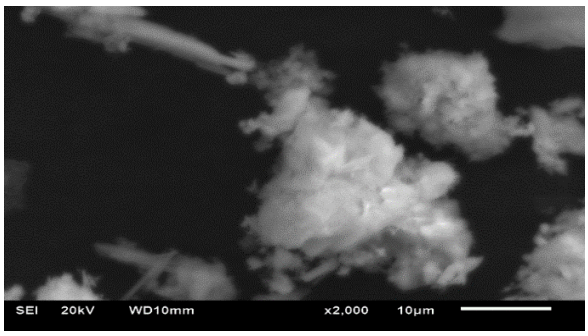

Figure 1

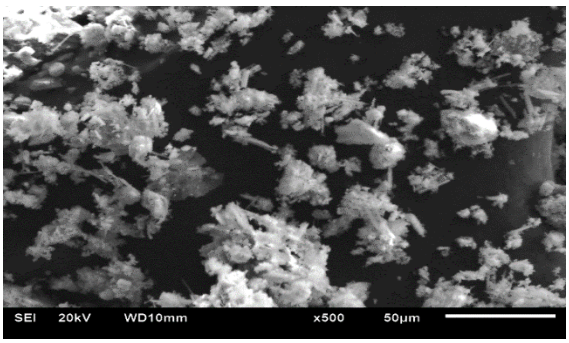

Figure 2

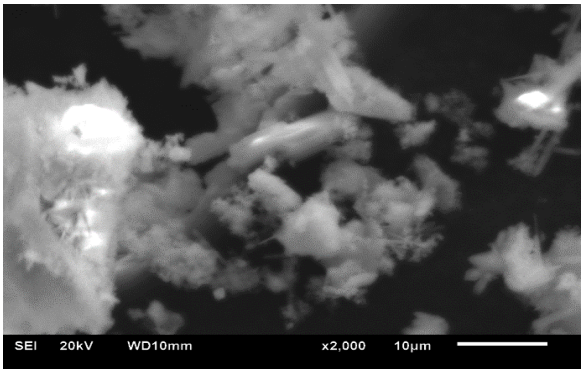

Figure 3

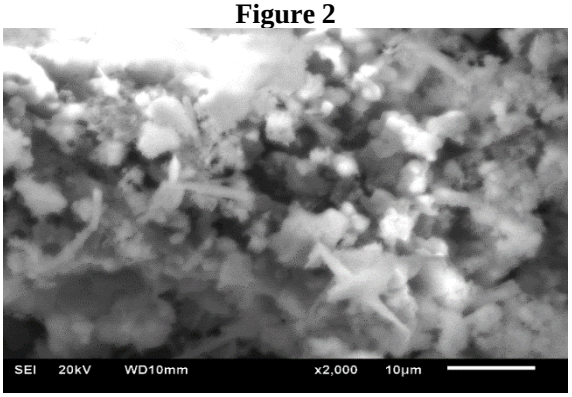

Figure 4

Fig. 1, 2, 3 and 4: SEM-Images of Nano-Zinc Oxide particles

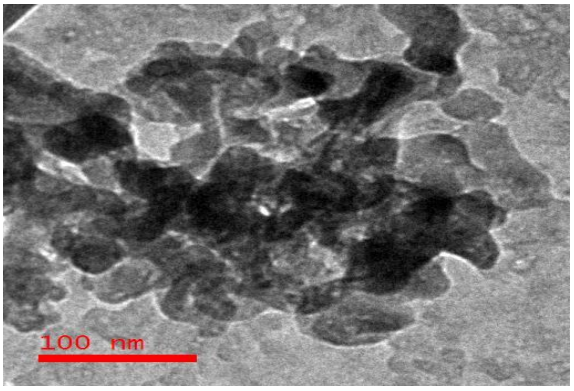

Figure 5

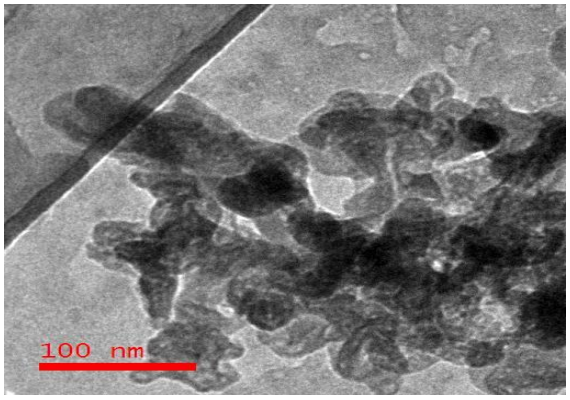

Figure 6

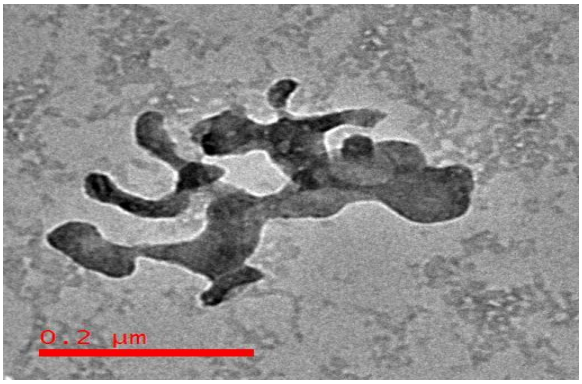

Figure 7

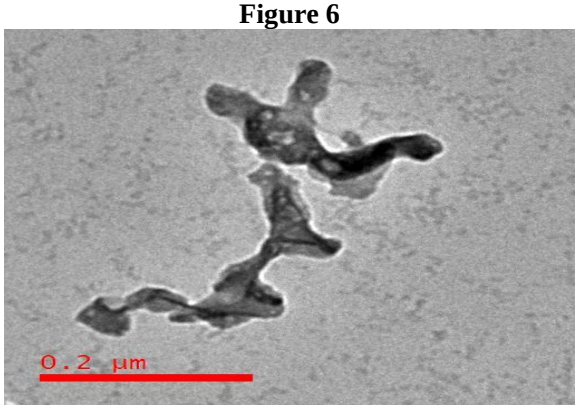

Figure 8

Fig. 5, 6, 7 and 8: TEM-Images of Nano-Zinc Oxide particles

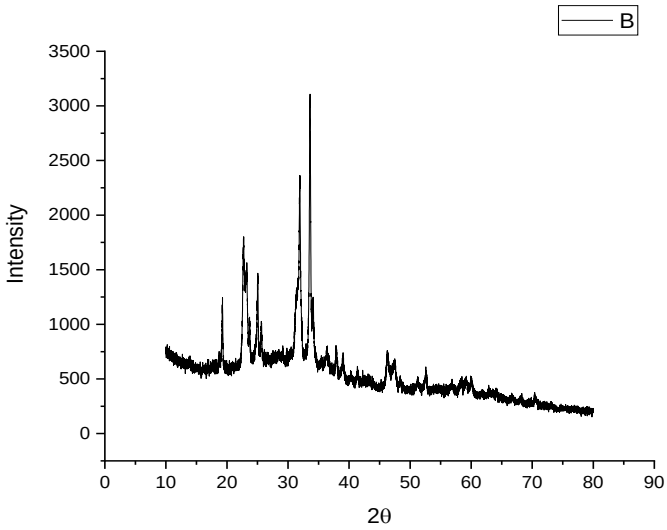

Fig. 9: X-ray Diffraction graph of Nano-ZnO particles

Table 1
Standards of FTIR spectroscopy

S.N.	IR values of Nano-zinc oxide	Obligation
1.	3434.96 cm^{-1}	Strong OH stretching vibrations
2.	1626.60 cm^{-1}	C=O stretching vibrations
3.	1384.20 cm-1	N-H stretching vibrations
4.	2800-3000 cm^{-1}	C-H Stretching vibrations
5.	1111.06 cm^{-1}	C-O single bond stretching vibrations
6.	600-720 cm^{-1}	C-H bending vibrations
7.	469 cm^{-1}	The peak of zinc oxide nanoparticles

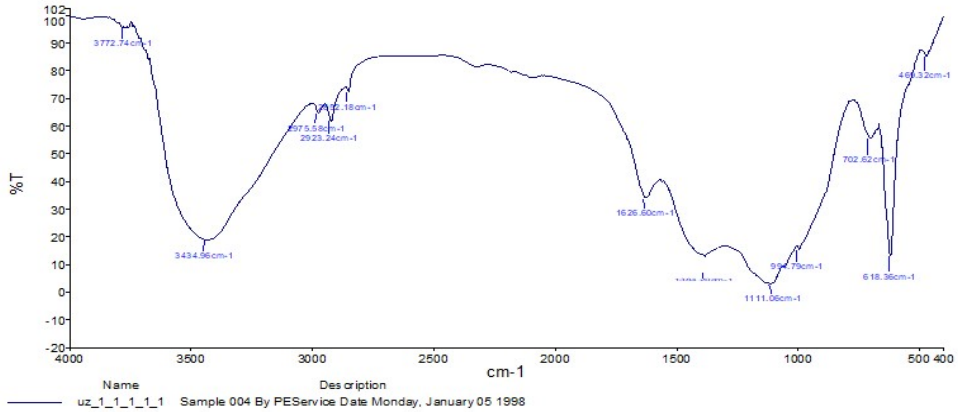

Wavenumber cm^{-1}

Fig. 10: FTIR Graph of Nano-ZnO particles

ZnO P. aeruginosa ZnO S. Pyogenes ZnO Klebsiella

Figures 11: Showing the zone of inhibition for ZnO NPs with *P. aeruginosa*, *S. Pyogenes* and *Klebsiella*

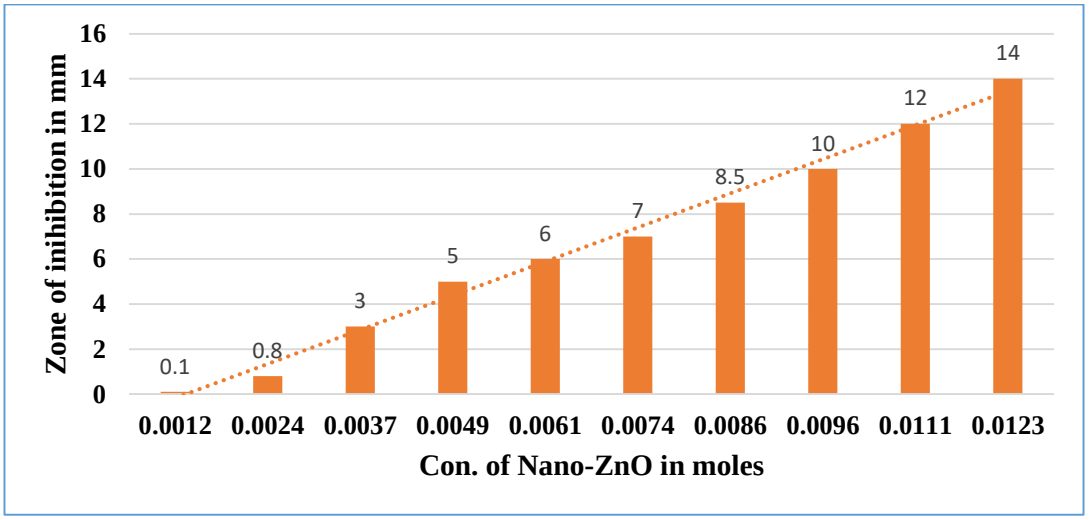

Fig. 12: Graph of Anti-Microbial activity with *P. Aeruginosa*

To assess bacterial activity, we prepared Nano-ZnO solutions at concentrations of 0.0012, 0.0024, 0.0037, 0.0049, 0.0061, 0.0074, 0.0086, 0.0096, 0.0111 and 0.0123 moles which correspond to 10, 20, 30, 40, 50, 60, 70, 80, 90 and 100 mg respectively. The three bacterial agar inoculums solidified in separate Petri plates. Wells measuring 7 mm in diameter were created on each agar Petri plate, into which 10 different doses of Nano-ZnO solution were introduced into the designated wells. Inhibition zones were assessed following a 24-hour incubation period at 37°C. The inhibitory zones for *P. aeruginosa* were measured at 0.1, 0.8, 3, 5, 6, 7, 8.5, 10, 12 and 14 mm, corresponding to concentrations of 10, 20, 30, 40, 50, 60, 70, 80, 90 and 100 mg. The zone values for *S. pyogenes* are recorded as 0.0, 0.5, 1.5, 2.7, 3.5, 5, 6, 7, 9 and 11 mm beginning at 10 mg, while for *Klebsiella*, the values are 0.0, 0.2, 0.7, 2, 3, 5.5, 7, 8.3, 9 and 10 mm starting from 10 mg, as presented in table 2. The data indicate that Nano-ZnO particles exhibit significant antibacterial activity, with *P. aeruginosa* demonstrating the highest levels, as illustrated in fig. 12, fig. 13 and fig. 14. Finally, fig. 11 shows the zone of inhibition for ZnO NPs with *P. aeruginosa*, *S. Pyogenes* and *Klebsiella*.

Table 2
Zone of inhibition standards of Anti-Microbial activity:

S.N.	Conc. of Nano-ZnO		Zone of inhibition in mm		
	In Moles	In mg	*P. aeruginosa*	*S. Pyogenes*	*Klebsiella*
1.	0.0012	10	0.1	0.0	0.0
2.	0.0024	20	0.8	0.5	0.2
3.	0.0037	30	3	1.5	0.7
4.	0.0049	40	5	2.7	2
5.	0.0061	50	6	3.5	3
6.	0.0074	60	7	5	5.5
7.	0.0086	70	8.5	6	7
8.	0.0096	80	10	7	8.3
9.	0.0111	90	12	9	9
10.	0.0123	100	14	11	10

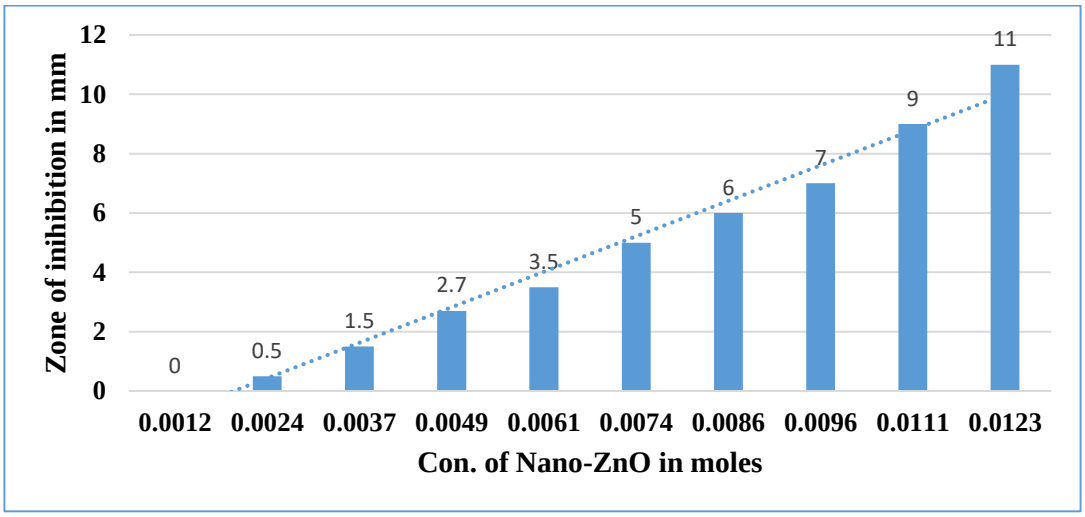

Fig. 13: Graph of Anti-Microbial activity with *S. Pyogenes*

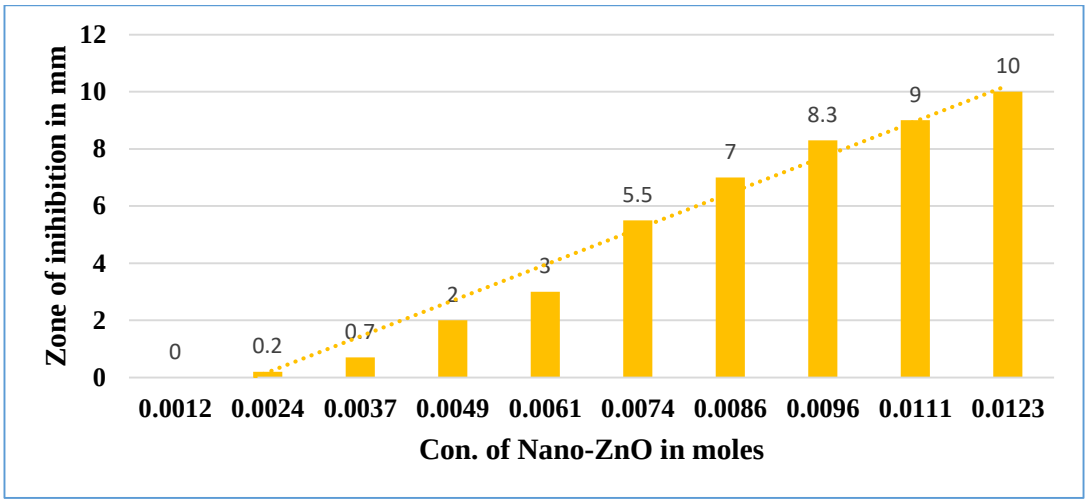

Fig. 14: Graph of Anti-Microbial activity with *Klebsiella*

Conclusion

This study of the CR method employed to synthesize nano-ZnO particles demonstrated that this approach produces nanoparticles of reduced size and in larger quantities, while effectively minimizing waste. The challenging aspect here involves employing SEM and TEM techniques to ascertain the 100 nm dimensions, surface morphology and topology of ZnO NPs. We verified and established that the FTIR spectrum data show a peak at 469 cm^{-1}, corresponding to the stretching frequency of Zn NPs, which is used for characterizing the crystalline phase through XRD analysis. The nano ZnO particles exhibit a significantly smaller size and demonstrate superior antibacterial activity in comparison to commercial zinc materials. The ZnO

nanoparticles exhibit significant antimicrobial efficacy against P. aeruginosa, S. pyogenes and Klebsiella, with P. aeruginosa demonstrating the highest activity, showing a 14 mm zone of inhibition when treated with 100 mg of Zn nanoparticles, in contrast to the other two bacterial strains.

Acknowledgement

We would like to express our sincere gratitude to Department of Chemistry, Koneru Lakshmaiah Education Foundation, Guntur-522502, Andhra Pradesh, India, for providing all the facilities during this research work.

References

1. Abdolhoseinzadeh A. and Sheibani S., The enhanced photocatalytic performance of Cu2O nano-photocatalyst powder was modified by ball milling and ZnO, *Adv. Powder Technol.*, **31(1)**, 40-50 **(2020)**

2. Hernández R., Hernández-Reséndiz J.R., Martínez-Chávez A., Velázquez-Castillo R., Escobar-Alarcón L. and Esquivel K., Au-TiO2 Synthesized by a Microwave- and Sonochemistry-Assisted Sol-Gel Method: Characterization and Application as Photocatalyst, *J. Sol-Gel Sci. Technol*., **10(9)**, 1052–1069 **(2020)**

3. Kołodziejczak-Radzimska A. and Jesionowski T., Zinc Oxide—From Synthesis to Application: A Review, *Materials*, **7(4)**, 2833–2881 **(2014)**

4. Kusuma U.R.S., Bhat S.V. and Vinayak K., On exceeding the solubility limit of Cr+3 dopants in SnO_2 nanoparticles-based dilute magnetic semiconductors. *J. Appl. Phys.*, **123(16)**, 161518-161524 **(2018)**

5. Matthew E. et al, Pyroelectric Properties of PVDF: MWCNT Nanocomposite Film for Uncooled Infrared Detectors, *Mater. Sci. Appl.*, **3(12)**, 851–855 **(2012)**

6. Mazhdi M. and Tafreshi M.J., The effects of gadolinium doping on the structural, morphological, optical and photoluminescence properties of zinc oxide nanoparticles prepared by co-precipitation method, *Appl. Phys. A.*, **124(12)**, 863–871 **(2018)**

7. Nagarajan P. and Rajagopalan V., Enhanced bioactivity of ZnO nanoparticles and antimicrobial study, *Sci. Technol. Adv. Mater*., **9(3)**, 035004–035012 **(2008)**

8. Patil B.N. and Taranath T.C., Limonia acidissima L., leaf-mediated synthesis of zinc oxide nanoparticles: A potent tool against Mycobacterium tuberculosis, *Int. J. Mycobacterial*., **115**, 227-232 **(2016)**

9. Rajendran S., Kandasamy S. and Rajendran, Synthesis and Characterization of Zinc Oxide and Iron Oxide Nanoparticles Using Sesbania Grandiflora Leaf Extract as Reducing Agent, *J. Nanosci*., **2017**, 1–7 **(2017)**

10. Wang L. and Muhammed M., Synthesis of zinc oxide nanoparticles with controlled morphology, *J. Mater. Chem*., **9(11)**, 2871–2878 **(1999)**.

(Received 29th July 2025, accepted 06th September 2025)